Effect of loading rate and coating thickness on wear and adhesion during sliding indents of Si-C-N hard coatings deposited on glass substrates

A S Bhattacharyya[1,2]

[1]Department of Metallurgical and Materials Engineering, Central University of Jharkhand
[2]Centre of Excellence in Green and Efficient Energy Technology (CoE GEET, Central University of Jharkhand

October 20, 2023

Abstract

Scratch tests were done on thermally resistant hard Si-C-N coatings developed on glass substrates using magnetron sputtering. The change in loading rate and coating thickness showed variation in adhesion strength and wear, The Boussinesq, Hans and Blister stress distribution beneath the indenter had on effect of the failure processes. Elastic recovery was prevalent in coatings of higher thickness and higher rate of loading. The increased loading rate although caused early failure but resulted in less wear.

Effect of loading rate and coating thickness on wear and adhesion during sliding indents of Si-C-N hard coatings deposited on glass substrates

A.S. Bhattacharyya [1, 2 §]

[1]Department of Metallurgical and Materials Engineering, Central University of Jharkhand, Ranchi: 835205, India
[2]Centre of Excellence in Green and Efficient Energy Technology (CoE GEET)
Central University of Jharkhand, Ranchi: 835205, India

§Corresponding author:
2006asb@gmail.com, arnab.bhattacharya@cuj.ac.in

ABSTRACT
Scratch tests were done on thermally resistant hard Si-C-N coatings developed on glass substrates using magnetron sputtering. The change in loading rate and coating thickness showed variation in adhesion strength and wear, The Boussinesq, Hans and Blister stress distribution beneath the indenter had on effect of the failure processes. Elastic recovery was prevalent in coatings of higher thickness and higher rate of loading. The increased loading rate although caused early failure but resulted in less wear.

Keywords: Scratch, hard coatings, Si-C-N, glass, loading rate, wear

INTRODUCTION
Si-C-N coatings were initially developed as a polymer-derived ceramic and have proven to be highly useful at high temperatures. [1]. They operate as a barrier to the environment's high temperatures and chemical damaging effects, preserving the substrate beneath. [2, 3]. Si-C-N coatings on glass substrates have applications as optical devices, sensors [4-8] and even in the field of endodontics [9]. An effect of substrate temperature on the adhesive strength of Si-C-N on various substrates including glass has been previously reported [10]. An effect of loading rate on the ductile-brittle failure mode has been reported [11].

In the scratch test, the stress field is a combination of Boussinesq (σ_{Bous}) from indenter loading, which has two components, normal and tangential, and Blister (Blister) from residual stress. The normal component of σ_{Bou} is substituted with Hans field (σ_{Hans}) in conical indenters. These fundamental stresses are also connected to shear components. [12, 13].

At the critical load (**Lc**), where adhesive failure occurs, the tractional force curve exhibits a quick and noticeable slope change. [14]. In case of Rockwell C, the initial contact being spherical, σ_{Bous} is active, but gets replaced by σ_{Hans} as the scratch progresses. The $\sigma_{Blister}$ on the other hand is coating thickness dependent. A higher coating thickness will lead to increase in its percentage causing higher material removal (wear) post adhesive failure.

An attempt has been made in this communication to address the changing loading rate (R_L) in the sliding indentation (scratch) process and coating

thickness (affecting residual stress) getting reflected in the adhesive failure and wear of the technologically important hard coatings deposited on glass substrates.

MATERIALS & METHODS
Magnetron sputtering (HHV, Bangalore, India) was used to deposit Si-C-N coatings on glass substrates at in an Ar/N₂ environment from a SiC target. Scratch Test Tr-101 (Ducom, Bangalore, India) was used to perform the sliding indents, which used a Rockwell C indenter. The scratch tests were done at rate of **5** and **2 N/mm** at a speed of **0.2 mm/s**. ImageJ software was used to get profiles of the scratch tracks.

RESULTS & DISCUSSIONS
The normal applied ramping load and the responsive tractional force vs. scratch length curves obtained during tests on coatings placed on glass substrates of thickness **0.5** and **3.9 µm** for **2N/mm** and **5N/mm** loading rates are shown in *Figs. 1-4*. A complete brittle failure is evident from absence of any slope of the tractional force. The formation of debris and spallation occurring can be related to the wear taking place during the scratching process. An increased and early brittle failure is indirect evidence of poor adhesion [15].

In *Fig 1 (a)*, the failure of the film starts at **0.5mm** at a load of **7 N** (lower critical load) indicating cohesive failure. Considering the indenter diameter of **200 µm**, the Boussinesq/ Hans stress is **159 MPa** imposed by the indenter. The coating breakdown becomes more and more severe with increase in normal load evident from the rise in amplitude of vibration of the tractional force curve

Severe brittle failure accompanied by coating removal started at the upper critical load (**Lc**) of **10 N** evident from the high and low amplitudes of the curve. The image of the scratch track showed brittle failure *(Fig1b)*. The material removal can be quantified by means of the height × width percentage (hw = 36) of the linear profile of the marked region. The specific wear rate WR$_s$ is given as **eq 1a**, which is equivalent to **eq 1b** where t is the scratch length (**5 mm**). The value comes out as **3.6×10⁻³ mm²/N**

$$WR_S = \frac{Volume\ Loss}{Load\ .\ sliding\ distance} \quad \textbf{(1a)}$$

$$WR_S = \frac{(hw)\ t}{R\ _L} \quad \textbf{(1b)}$$

The coating thickness of **0.5µm** contributes to the σ$_{Blister}$. Tensile stress promotes adhesive failure by chipping, whereas compressive stress aids in the creation of fissures. A modified variation of Stoney's equation, as provided in **eq 2**, can be utilized for coating substrate systems [16[.

$$\sigma t \sim \sigma_{Blister} = p\ ln\left(\frac{KEh^2}{6p(1-v)} + 1\right) \ where\ p = \frac{h^3}{D^2}E\left(\frac{13\cdot5}{1-v^2} - 10.3\right) \quad \textbf{(2)}$$

h is the thickness of the whole film/substrate system, and t is the thickness of the coating. The parameter D is the diameter of the coating when the shape is circular, and it is set to **0.2 mm**, which is the diameter of the spherical Rockwell C indenter. The deposited layer had a thickness of **0.5 μm** on a **1 mm** thick Si substrate. As a result, h is taken to be 1 mm. The stiffness is defined as **0.1 mN/nm (MN/m)** divided by the value of k, the spring constant. The value of $\sigma_{Blister}$ is the surface stress which is about 300 MPa. These stresses affect the nature of the failure. As the shear component of stress is equally significant for the coating system, the parameter h on being replaced by t only will provide $\tau_{Blister}$ as **21MPa**.

Fig 2a shows a lower critical load of **2.5 N** (cohesive failure) and an upper critical load of **8 N** (adhesive failure) of 0.5 μm coatings on glass for a lower R_L of **2N/mm**. The scratch micrograph shows a sudden and brittle nature of film failure. However, the failure amplitudes as observed in the tractional force curve are less severe due to the lower loading rate of **2N/mm** compared to **5N/mm** in the previous case. A clear indication of adhesive failure can be seen in the optical image of the scratch track (*Fig 2b*). The cross-section profile of scratch track prior and post adhesive failure are given in *Fig 2c, d* respectively. The specific wear rate (WRs) was **3.6 ×10⁻³ mm²/N** which was same as the previous case of higher R_L.

An interesting observation however prevailed with the intensity of coating delamination vertically getting reduced after an initial zone of enhanced detachment as marked in *Fig 2b*. The reason behind this observation was the strain energy being accumulated with the initiation of the scratch suddenly gets released as the coating starts to fail and the rate of release saturates to some extent thereafter.

The films showed an initial failure at **13N** at a sliding distance of **1mm** for a loading rate of **2N/mm** for coatings of higher thickness **(3.9μm)** (*Fig 3a*). Film failure by *wedge spallation* is seen (*Fig 3b)* after an adhesive critical load of **17N.** The cross-sectional line profile showed a hw of 84 indicating high material loss and wear rate of **163.8 ×10⁻³ mm²/N**

Increasing the R_L to **5N/mm** showed a localized film failure where the groove continued to exist even after an initial film failure (*Fig 4a, b*). The higher rate of loading was able to cause an elastic recovery after the failure due to increase coating thickness. Correspondingly, the wear was also less (58.5 ×10⁻³ **mm²/N).** The main failed regions in the scratch track were surrounded delaminated regions which were due to
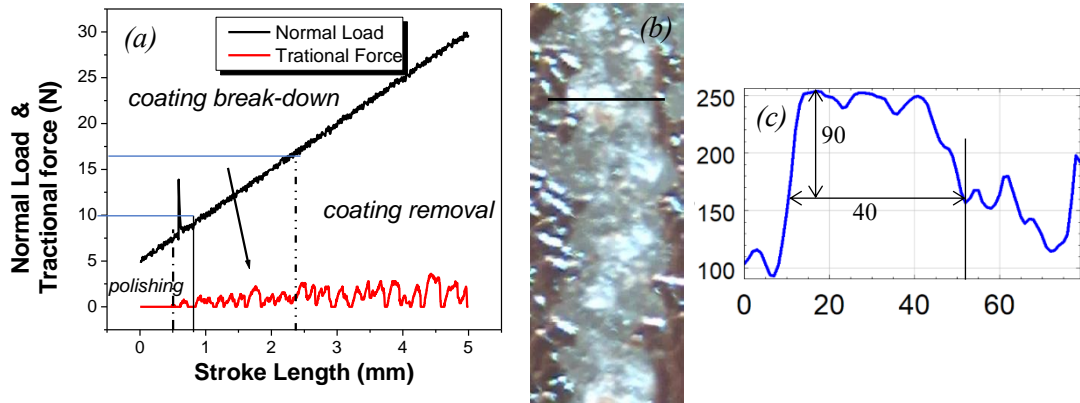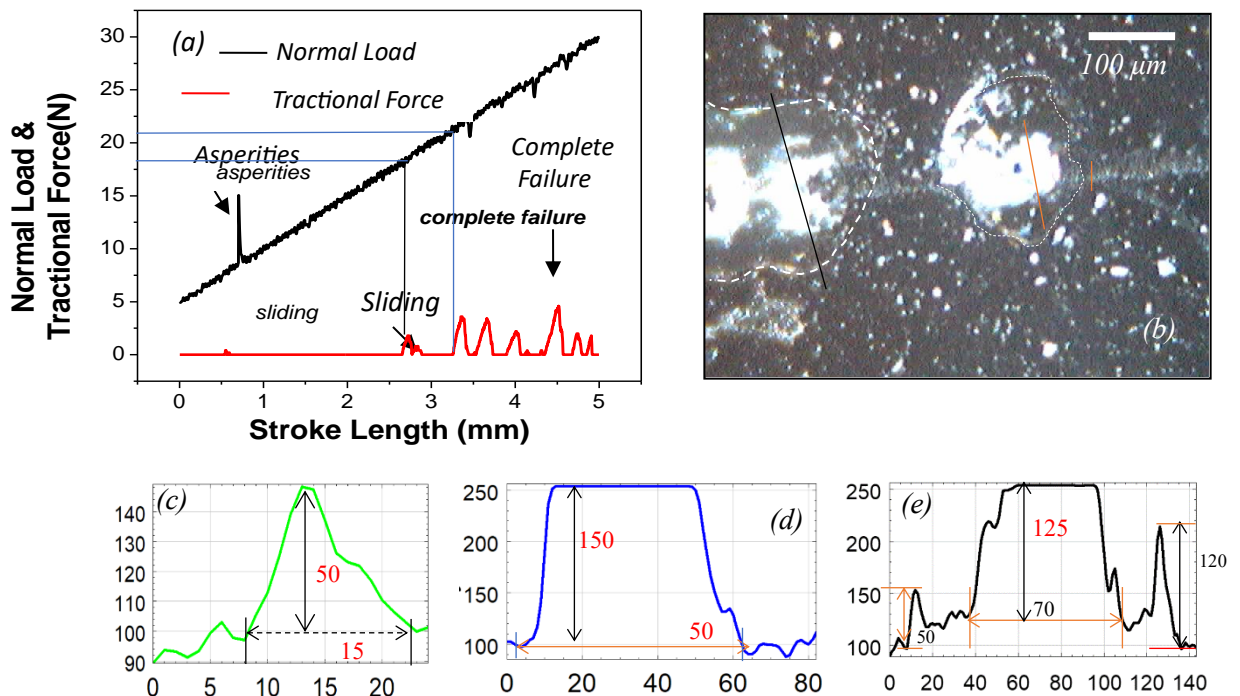
Fig 1: Scratch tests with **5N/mm** loading rate for glass substrates showing plots of (a) Normal load and Tractional force vs. stroke length and (b) the optical micrograph of the scratch track (c) line profile of the scratch track showing material removal for a thickness of **0.5μm** [14]
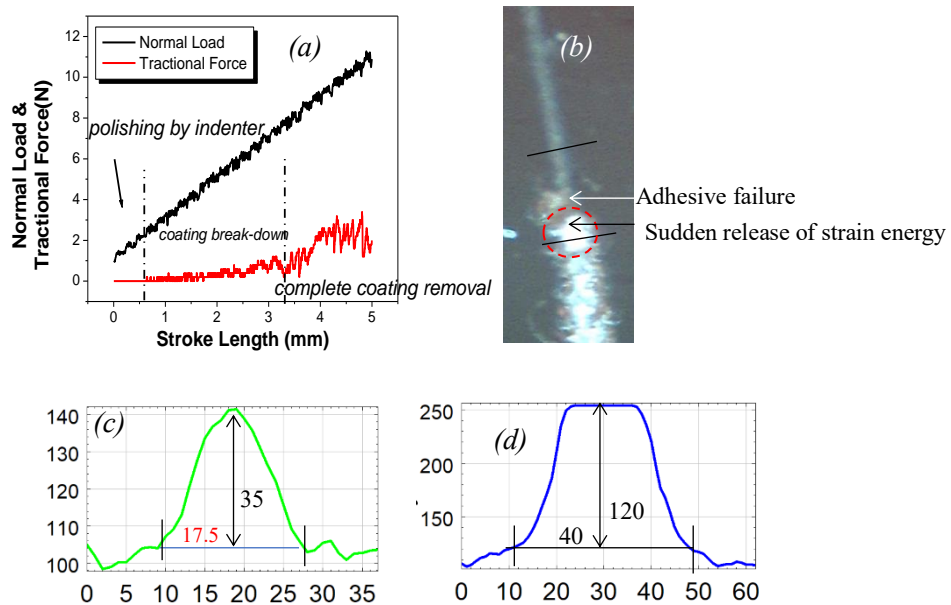
Fig 2: Scratch tests with **2N/mm** loading rate for glass substrates showing plots of (a) Normal load and Tractional force vs. stroke length and (b) the optical micrograph of the scratch track showing adhesive failure at **8 N**. (c) line profile of scratch track prior adhesive failure (d) post adhesive failure for thickness of **0.5μm** [14]
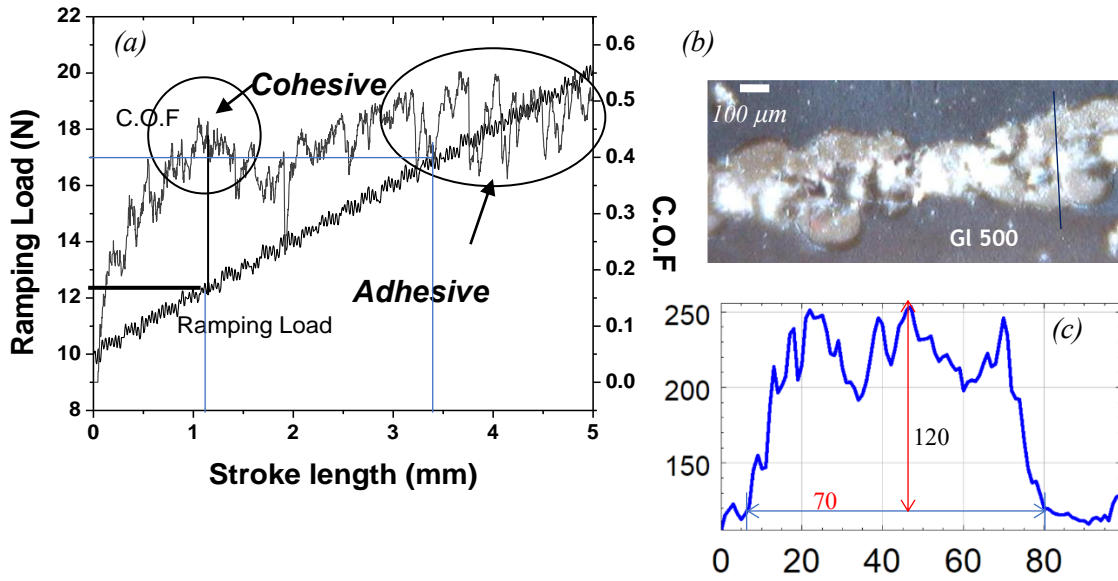
Fig 3: Scratch with **2N/mm** loading rate for glass substrates showing plots of (a) Normal load and C.O.F vs. stroke length and (b) the optical micrograph of the scratch track showing failure at **12 N (c)** line profile of the scratch region for a thickness of **3.9 μm[14]**
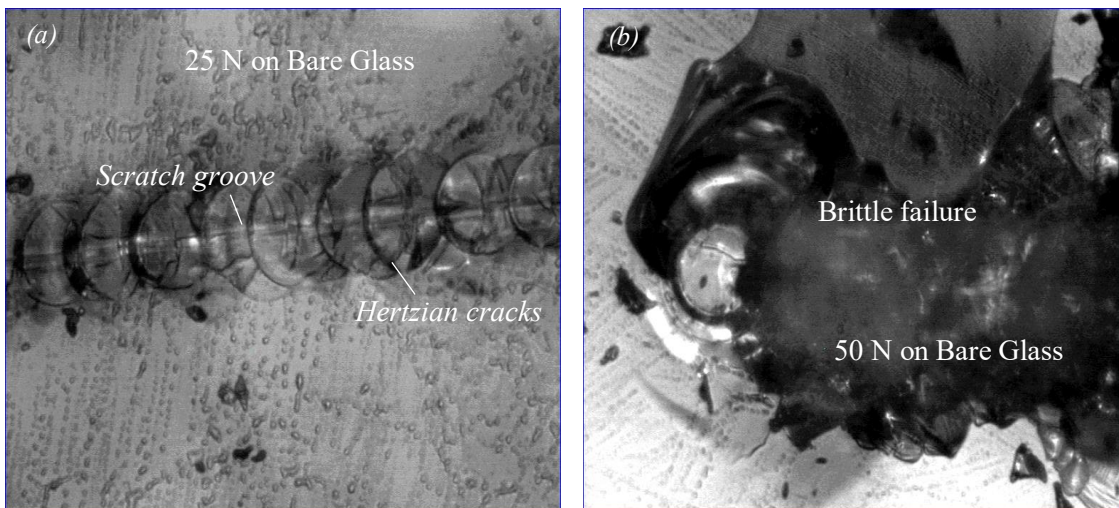

Fig 4: Scratch tests with **5N/mm** loading rate for glass substrates showing plots of (a) Normal load and Tractional force vs. stroke length and (b) the optical micrograph of the scratch track(c) linear profile of scratch track before failure (d) after first failure and (e) after second failure for a thickness of **3.9μm [14]**

A summary of the observations made with the change in loading rate and coating thickness is given in **Table 1**. Although thicker coatings showed higher Lc, they experience more Wear after adhesive failure. An increased loading rate gave higher critical load. An increased coating thickness showed more wear due to higher residual stress. An elastic recovery was also more likely to occur in thicker films. Scratch tests performed on bare glass substrates at 25N showed formation of Hertzian cracks with diameter matching with the spherical indenter tip diameter (*Fig 5a*). The scratch groove was also clearly observed. A catastrophic brittle failure was observed for 50 N load (*Fig 5b*).

Table 1. Effect of loading rate and coating thickness

$t(\mu m)$	R_L (N/mm)	Material loss (hw)	$L_{c\,1}$ (N)	$L_{c\,2}$ (N)	WRs $\times 10^{-3}$ (mm^2/N)
0.5	2	36	2.5	8	3.6
0.5	5	36	10	17	3.6
3.9	2	84	13	17	163.8
3.9	5	75	18	21	58.5

Fig 5. Scratch test with 25 N load showing circular Hertzian cracks and (b) complete brittle failure for 50N load on bare glass substrate.

CONCLUSIONS

A mixed response of coating thickness and loading rate was shown. Higher elastic recovery was observed with loading rate for coatings of higher thickness. Wear or loss of material was more with lower rate of loading. The Boussinesq, Blister (residual), and Hans (conical indenter) fields varied in different

conditions and manifested themselves into the different failure natures. Although the increased loading rate resulted in early failure, it resulted in less wear.

DECLARATIONS

Compliance with Ethical Standards
The manuscript has not been submitted in parallel either in full or partially to any other journal.

Conflict of interest
There is no conflict of interest among the authors

Research Data Policy and Data Availability Statements
Data shall be provided on request

Credit author statement
A. S. Bhattacharyya being the sole author, was involved in performing the experiments, analysing, and framing the manuscript

REFERENCE
1. Riedel, R.; Kleebe, H.-J.; Schönfelder, H.; Aldinger, F. A Covalent Micro/Nano-Composite Resistant to High-Temperature Oxidation. Nature 1995, 374 (6522), 526–528. https://doi.org/10.1038/374526a0.
2. A.S. Bhattacharyya, G.C. Das, S. Mukherjee, S.K. Mishra, Effect of radio frequency and direct current modes of deposition on protective metallurgical hard silicon carbon nitride coatings by magnetron sputtering, *Vacuum*,83, 12, 2009, 1464-1469, https://doi.org/10.1016/j.vacuum.2009.06.051.
3. Mishra, S. K.; Bhattacharyya, A. S.; Rupa, P. K. P.; Pathak, L. C. XPS Studies on Nanocomposite Si–C–N Coatings Deposited by Magnetron Sputtering *Nanoscience and Nanotechnology Letters,* 4, 3, 2012, 352-357https://doi.org/10.1166/nnl.2012.1320
4. Peng, Yinqiao, Jicheng Zhou, Baoxing Zhao, Xiaochao Tan, and Zhichao Zhang. "Structural and optical properties of the SiCN thin films prepared by reactive magnetron sputtering." *Applied Surface Science* 257, no. 9 (2011): 4010-4013.
5. Park, N.M., Kim, S.H. and Sung, G.Y., 2003. Band gap engineering of SiCN film grown by pulsed laser deposition. *Journal of applied physics*, *94*(4), pp.2725-2728.
6. Wu, X.C., Cai, R.Q., Yan, P.X., Liu, W.M. and Tian, J., 2002. SiCN thin film prepared at room temperature by rf reactive sputtering. *Applied surface science*, *185*(3-4), pp.262-266.
7. Wrobel, Aleksander M., and Pawel Uznanski. "Amorphous silicon carbonitride (a-SiCN) thin film coatings by remote plasma chemical vapor deposition using organosilicon precursor: Effect of substrate temperature." *Plasma Processes and Polymers* 20, no. 4 (2023): 2200190.
8. Li, Lanlan, Yingping He, Lida Xu, Chenhe Shao, Gonghan He, Daoheng Sun, and Zhenyin Hai. "Oxidation and Ablation Behavior of Particle-Filled SiCN Precursor Coatings for Thin-Film Sensors." *Polymers* 15, no. 15 (2023): 3319.
9. Xia, Xinyi, Chao-Ching Chiang, Sarathy K. Gopalakrishnan, Aniruddha V. Kulkarni, Fan Ren, Kirk J. Ziegler, and Josephine F. Esquivel-Upshaw. "Properties of SiCN Films Relevant to Dental Implant Applications." *Materials* 16, no. 15 (2023): 5318.
10. Mishra, Suman K., and A. S. Bhattacharyya. "Effect of substrate temperature on the adhesion properties of magnetron sputtered nano-composite Si–C–N hard thin films." Materials Letters 62, no. 3 (2008): 398-402.
11. A S Bhattacharyya. Dual mode fracture based on loading rate during sliding indentation of Si-C-n hard coatings on 304S substrates. *Authorea.* October 19, 2023. 10.22541/au.169774192.22359266/v1
12. Qian, H.; Chen, M.; Qi, Z.; Teng, Q.; Qi, H.; Zhang, L.; Shan, X. Review on Research and Development of Abrasive Scratching of Hard Brittle Materials and Its Underlying Mechanisms. *Crystals* 2023, *13*, 428. https://doi.org/10.3390/cryst13030428

13. Lv, B.; Lin, B.; Sui, T.; Liu, C. Crack Extension Mechanism and Scratch Stress Field Model of Hard and Brittle Materials Caused by Curvature Effect. *J. Mater. Process. Technol.* 2023, *319* (118058), 118058. https://doi.org/10.1016/j.jmatprotec.2023.118058.

14. Mishra, S.K., Bhattacharyya, A.S. (2013). Adhesion and Indentation Fracture Behavior of Silicon Carbonitride Nanocomposite Coatings Deposited by Magnetron Sputtering. In: Li, H., Wu, J., Wang, Z. (eds) Silicon-based Nanomaterials. Springer Series in Materials Science, vol 187. Springer, New York, NY. https://doi.org/10.1007/978-1-4614-8169-0_10

15. Kabir, M. S.; Zhou, Z.; Xie, Z.; Munroe, P. Scratch Adhesion Evaluation of Diamond like Carbon Coatings with Alternate Hard and Soft Multilayers. *Wear* 2023, *518–519* (204647), 204647. https://doi.org/10.1016/j.wear.2023.204647.

16. H. Liu, M. Dai, X. Tian, S. Chen, F. Dong, L. Lu Modified Stoney formula for determining stress within thin films on large-deformation isotropic circular plates, AIP Advances 11, 125009 (2021)